Journal of Engineering Mathematics **29:** 413–436, 1995.

Stable pattern and standing wave formation in a simple isothermal cubic autocatalytic reaction scheme

R. HILL[1], J.H. MERKIN[1] and D.J. NEEDHAM[2]
[1]*Department of Applied Mathematics, University of Leeds, Leeds, LS2 9JT, United Kingdom*
[2]*School of Mathematics, University of East Anglia, Norwich, NR4 7TJ, United Kingdom*

Received 10 March 1994; accepted in revised form 29 December 1994

Abstract. The formation of stable patterns is considered in a reaction-diffusion system based on the cubic autocatalator, $A + 2B \rightarrow 3B$, $B \rightarrow C$, with the reaction taking place within a closed region, the reactant A being replenished by the slow decay of precursor P via the reaction $P \rightarrow A$. The linear stability of the spatially uniform steady state $(a, b) = (\mu^{-1}, \mu)$, where a and b are the dimensionless concentrations of reactant A and autocatalyst B and μ is a parameter representing the initial concentration of the precursor P, is discussed first. It is shown that a necessary condition for the bifurcation of this steady state to stable, spatially non-uniform, solutions (patterns) is that the parameter $D < 3 - 2\sqrt{2}$ where $D = D_b/D_a$ (D_a and D_b are the diffusion coefficients of chemical species A and B respectively). The values of μ at which these bifurcations occur are derived in terms of D and λ (a parameter reflecting the size of the system). Further information about the nature of the spatially non-uniform solutions close to their bifurcation points is obtained from a weakly nonlinear analysis. This reveals that both supercritical and subcritical bifurcations are possible. The bifurcation branches are then followed numerically using a path-following method, with μ as the bifurcation parameter, for representative values of D and λ. It is found that the stable patterns can lose stability through supercritical Hopf bifurcations and these stable, temporally periodic, spatially non-uniform solutions are also followed numerically.

1. Introduction

Cubic autocatalysis has been shown to form the key step in a number of complex reaction schemes, see, for example, the review lecture of Gray [1]. In particular, Hanna *et al.* [2] and Saul and Showalter [3] have demonstrated that cubic autocatalysis provides a good model for the iodate – arsenous acid reaction. The mechanism of cubic autocatalysis also has similarities with many models arising in mathematical biology, see, for example, that given originally by Schnakenberg [4] which has been discussed by Murray [5, 6] and Acuri and Murray [7]. This rate law has also been suggested for enzyme reactions (glycosis), Sel'kov [8].

In this paper we consider the prototype chemical reaction scheme based on the cubic autocatalator,

$$A + 2B \rightarrow 3B \qquad \text{rate } k_1 \bar{a}\bar{b}^2, \tag{1}$$

$$B \rightarrow C \qquad \text{rate } k_2 \bar{b}, \tag{2}$$

where $\bar{a}$ and $\bar{b}$ are the concentrations of the reactant A and the autocatalyst B and the k_i are rate constants (both reactions are assumed to be isothermal). It has been shown that the reaction scheme given by (1) and (2) can, in an open system (the c.s.t.r.), exhibit a range of complex behaviour, see, for example, D'Anna *et al.* [9], Gray and Scott [10, 11, 12, 13] and Gray and Roberts [14]. Here we suppose that the reaction is taking place inside a closed

system with the reactant A now being replenished by the slow decay of a precursor P, via the simple isothermal step,

$$P \rightarrow A \qquad \text{rate } k_0\bar{p}. \tag{3}$$

where $\bar{p}$ is the concentration of reactant P. The reaction scheme (1)–(3) has been discussed in some detail for a well-stirred system (*i.e.* one with no spatial variations), allowing for the slow decay of the precursor P, Merkin *et al.* [15] and also under the "pool chemical", approximation (where the concentration of P is assumed to remain constant throughout), Merkin *et al.* [16]. The slow uncatalysed reaction step $A \rightarrow B$ can have a substantial effect on the overall reaction, and this has been discussed by Merkin *et al.* [17], again for the well-stirred system.

In the present paper, we consider the reaction scheme (1)–(3) taking place inside a closed vessel *without stirring*. This allows for spatial variations in the reactant concentrations throughout the vessel, arising via the combined mechanisms of reaction and molecular diffusion. The development and propagation of reaction-diffusion waves from initially non-homogeneous distributions of reactants for this scheme has been considered by Merkin and Needham [18]. Also the formation of partially stable (transient) spatial and temporal pattern forms for this scheme has been studied by Needham and Merkin [19]. In both of these papers it was assumed throughout that the diffusion coefficients for the species A and B are equal. This assumption is plausible for many chemical reaction schemes for which (1)–(3) provide a basis, where the diffusion coefficients of the two species represented by A and B are of a comparable order of magnitude. However, in many biological contexts, for example in enzyme reactions, the diffusion coefficients may differ more significantly between species. The aim of the present paper is to study the effects on stability and pattern formation in the reaction scheme (1)–(3) when the diffusion coefficients of the species A and B are unequal.

As in [19], for analytical convenience, we restrict the spatial variation to one dimension, and measure distance in this dimension with the coordinate $\bar{x}$. The vessel is taken to have length l with impermeable boundaries at $\bar{x} = 0, l$. Physically this will model a thin layer of reacting material confined in a vessel which is much longer than its width.

The equations governing the evolution in concentration of the reactants in the vessel are, as in [19],

$$\left.\begin{aligned} \frac{\partial \bar{p}}{\partial \bar{t}} &= D_p \frac{\partial^2 \bar{p}}{\partial \bar{x}^2} - k_0\bar{p}, \\ \frac{\partial \bar{a}}{\partial \bar{t}} &= D_a \frac{\partial^2 \bar{a}}{\partial \bar{x}^2} + k_0\bar{p} - k_1\bar{a}\bar{b}^2, \\ \frac{\partial \bar{b}}{\partial \bar{t}} &= D_b \frac{\partial^2 \bar{b}}{\partial \bar{x}^2} + k_1\bar{a}\bar{b}^2 - k_2\bar{b}. \end{aligned}\right\} \tag{4a}$$

Here D_i $(i = p, a, b)$ are constant diffusion coefficients and $\bar{t}$ is time. In addition to equations (4a) we have the boundary conditions associated with the impermeable walls, namely

$$\frac{\partial \bar{a}}{\partial \bar{x}} = \frac{\partial \bar{b}}{\partial \bar{x}} = \frac{\partial \bar{p}}{\partial \bar{x}} = 0 \qquad \text{on } \bar{x} = 0, l. \tag{4b}$$

Following [19], we consider the situation in which the precursor P is initially uniformly distributed throughout the vessel with constant concentration p_0. Thus we have the initial condition,

$$\bar{p}(\bar{x}, 0) = p_0, \quad 0 < \bar{x} < l. \tag{5}$$

In addition, the reaction kinetics are taken to satisfy the following scalings:

(i) the time scale associated with the decay of the precursor P in reaction (3) is much longer than the time scales associated with reaction steps (1) and (2).

(ii) the initial concentration, p_0, of the precursor P is large compared to typical concentrations of the intermediate species A and B.

To exhibit formally the simplifications available under these conditions, it is appropriate at this stage to introduce dimensionless quantities. Typical scales for $\bar{p}$ and $\bar{x}$ are clearly p_0 and l respectively. We denote typical scales for $\bar{a}$, $\bar{b}$ by a_s, b_s and a scale for $\bar{t}$ by t_s, which is to be based on the faster time scale associated with reactions (1) and (2). On balancing orders of magnitude for the production (or loss) of reactants A and B from reactions (1) and (2) over a time scale t_s, we deduce appropriate scales as,

$$a_s = b_s = \left(\frac{k_2}{k_1}\right)^{1/2}, \quad t_s = \frac{1}{k_2}. \tag{6}$$

These scales are then used to introduce the dimensionless quantities,

$$\bar{a} = a_s a, \quad \bar{b} = b_s b, \quad \bar{p} = p_0 p, \quad \bar{x} = lx, \quad \bar{t} = t_s t. \tag{7}$$

The resulting dimensionless equations governing the evolution of chemical species P, A and B are, from (4a) and (7),

$$\frac{\partial p}{\partial t} = \lambda_p \frac{\partial^2 p}{\partial x^2} - \sigma p \tag{8a}$$

$$\frac{\partial a}{\partial t} = \lambda_a \frac{\partial^2 a}{\partial x^2} + \mu p - ab^2 \tag{8b}$$

$$\frac{\partial b}{\partial t} = \lambda_b \frac{\partial^2 b}{\partial x^2} + ab^2 - b \tag{8c}$$

while conditions (4b) and (5) become

$$\frac{\partial p}{\partial x} = 0, \quad \frac{\partial a}{\partial x} = 0, \quad \frac{\partial b}{\partial x} = 0 \quad \text{at } x = 0, 1 \tag{9a}$$

$$p(x, 0) = 1, \quad 0 < x < 1 \tag{9b}$$

Here we have introduced the dimensionless parameters

$$\lambda_i = \frac{D_i}{k_2 l^2} \quad (i = p, a, b), \quad \sigma = \frac{k_0}{k_2}, \quad \mu = \frac{\sigma p_0}{a_s} \tag{10}$$

The λ_i give a measure of the relative rates of diffusion of the three species, σ compares the two reaction rates associated with the production and autocatalytic steps and the parameter μ measures the initial rate of production of A from P.

Assumption (i), (ii) above are the basis for the 'pool chemical' approximation, defined formally by

$$\sigma \ll 1 \text{ with } \mu = O(1) \text{ as } \sigma \to 0 \tag{11}$$

This limit will be taken for the subsequent analysis.

Equation (8a) can be integrated directly, subject to (9a,b), so that the concentration of the precursor P is everywhere given by,

$$p(x,t) = e^{-\sigma t}. \tag{12}$$

The precursor decays slowly and uniformly, producing the reactant A. It can therefore be eliminated from equation (8b) to leave,

$$\frac{\partial a}{\partial t} = \lambda_a \frac{\partial^2 a}{\partial x^2} + \mu e^{-\sigma t} - ab^2. \tag{13}$$

Equations (13) and (8c) show that at large times the system will settle to the chemical equilibrium solution where all the autocatalyst B has been converted to the final stable product C and a uniform residue of reactant A is left behind.

The real interest in this model is therefore to determine the transient features that can be observed before the final chemical equilibrium is achieved. Equation (13) shows that these transient features will be slowly varying over a time scale of $O(\sigma^{-1})$. Thus we may analyse this transient behaviour by making the "pool chemical" approximation in equation (13). This involves making the approximation $e^{-\sigma t} \simeq 1$, and studying the behaviour of solutions of the resulting autonomous equations for each constant value of $0 < \mu < \infty$. For each fixed μ, the resulting behaviour will then provide a good approximation to the slowly evolving transient behaviour over a time scale of $O(\sigma^{-1})$. This has been shown to be the case for the well-stirred (spatially uniform, i.e. putting $\lambda_a = \lambda_b = 0$) version of the equations, [15]. In [15] it was seen that, provided σ was sufficiently small, the system behaved "quasi-statically", i.e. the response of the system at a particular value of t was the same as that determined under the pooled chemical approximation [16] for the corresponding value of $\mu e^{-\sigma t}$ (treated as though this were a constant). The only differences between the "slowly decreasing μ" and the "constant μ" cases were seen near bifurcations in the latter case, which required in the former case a finite time for the solution to adjust to a new bifurcated solution state.

Under the "pool chemical" approximation the equations governing the concentrations a, b become,

$$\frac{\partial a}{\partial t} = \lambda_a \frac{\partial^2 a}{\partial x^2} + \mu - ab^2 \tag{14a}$$

$$\frac{\partial b}{\partial t} = \lambda_b \frac{\partial^2 b}{\partial x^2} + ab^2 - b \tag{14b}$$

with the boundary conditions

$$\frac{\partial a}{\partial x} = \frac{\partial b}{\partial x} = 0 \quad \text{at } x = 0, 1 \tag{14c}$$

and suitable initial conditions.

Earlier work on this system [18, 19] made the further simplification $\lambda_a = \lambda_b = \lambda$, requiring that the species A, B have diffusion coefficients that are (approximately) equal. For small molecules this is a sensible choice as very little variation is found between diffusion rates. However for reactions involving larger molecules, such as enzyme reactions, it is important to allow for different diffusion rates and in this context a factor of ten difference is not unreasonable. It is also worth noting that the autocatalytic scheme (14) has many similarities

with biological mechanisms where the rates of diffusion of the species may differ considerably, see for example Arcuri and Murray [7].

The governing equations (14) have been studied extensively for the spatially uniform case, [16], and it is instructive at this point to summarize these results before analysing the full equations. There are three ranges of μ to consider.

(i) $1 \leqslant \mu < \infty$

The only locally stable states of the system are the unique steady state S

$$a \equiv \mu^{-1}, \quad b \equiv \mu,$$

and the conversion state C,

$$a \equiv \mu t + \alpha, \quad b \equiv 0,$$

(with α an arbitrary constant), whereby all the autocatalyst has been depleted via step (2) and only the constant production of A from the precursor P via step (3), with P at its initial concentration p_0 under the pooled chemical approximation, remains.

At $\mu = 1$ the steady state S loses its stability through a supercritical Hopf bifurcation, which leads to the creation of a stable limit cycle L in $\mu < 1$. The steady state Ss remains unstable for each $0 < \mu < 1$, while the limit cycle L increases in amplitude, without bound as $\mu \to \mu_h \simeq 0.90032$, when it is terminated at a heteroclinic bifurcation on equilibrium points at infinity. The conversion state C remains stable for all $0 < \mu < 1$. Thus we have,

(ii) $\mu_h \leqslant \mu \leqslant 1$

The only locally stable states of the system are the conversion state C and the limit cycle state L.

(iii) $0 < \mu < \mu_h$

The only stable state of the system is the conversion state C.

In this paper the effects of diffusion are included. With equal diffusion coefficients, $\lambda_a = \lambda_b$, it has been shown [19] that the uniform steady state S remains locally stable for $\mu > 1$. While for $\mu < 1$ there is a sequence of Hopf and pitchfork bifurcations from the spatially uniform steady state S, all leading to partially stable spatially or spatiotemporal periodic solutions. Observations of these states would be at most transient and on a time scale much less than $O(\sigma^{-1})$. The spatially homogeneous states L and C remain as the only states which are locally, absolutely stable. The present analysis examines the effect on this situation of allowing for unequal diffusion rates. For small differences, the perturbation is regular and the situation is qualitatively unchanged. However, for differences in diffusion rates of $O(1)$, new features emerge.

We begin, in the next section, by analyzing the local stability of the uniform steady state S.

2. The Linearized Theory

Here we consider the temporal stability of the uniform steady state S when subject to a disturbance of small amplitude. We linearize about S by writing

$$a = \mu^{-1} + \bar{a}(x,t) + \cdots \quad b = \mu + \bar{b}(x,t) + \cdots \tag{15}$$

On substituting from (15) into (14a,b), and retaining only the leading order terms, we obtain

$$\left.\begin{aligned} \frac{\partial \bar{a}}{\partial t} - \lambda_a \frac{\partial^2 \bar{a}}{\partial x^2} + \mu^2 \bar{a} + 2\bar{b} = 0 \\ \frac{\partial \bar{b}}{\partial t} - \lambda_b \frac{\partial^2 \bar{b}}{\partial x^2} - \mu^2 \bar{a} - \bar{b} = 0 \end{aligned}\right\} \tag{16}$$

subject to boundary conditions

$$\frac{\partial \bar{a}}{\partial x} = \frac{\partial \bar{b}}{\partial x} = 0 \quad \text{on } x = 0, 1. \tag{17}$$

The solution to the initial-boundary value problem (16), (17) is readily obtained as, [19],

$$\begin{aligned} \bar{a}(x,t) &= \sum_{r=0}^{\infty} \left[A_r^+ \exp(\omega_+ t) + A_r^- \exp(\omega_- t)\right] \cos r\pi x \\ \bar{b}(x,t) &= \sum_{r=0}^{\infty} \left[B_r^+ \exp(\omega_+ t) + B_r^- \exp(\omega_- t)\right] \cos r\pi x \end{aligned} \tag{18}$$

for $0 < x < 1$, $t > 0$. Here $A_r^{\pm}$, $B_r^{\pm}$ $(r = 0, 1, 2, \ldots)$ are constants related to the Fourier cosine series expansion of the initial disturbance while

$$k_r = r\pi\sqrt{\lambda_a} \quad r = 0, 1, 2, \ldots \tag{19}$$

and $\omega_{\pm} = \omega_{\pm}(k_r; \mu)$ are the two roots of the quadratic dispersion relation,

$$\omega^2 + p(\mu, k_r)\omega + q(\mu, k_r) = 0 \tag{20}$$

with,

$$p(\mu, k_r) = (1 + D)k_r^2 + \mu^2 - 1, \tag{21a}$$

$$q(\mu, k_r) = Dk_r^4 + (D\mu^2 - 1)k_r^2 + \mu^2. \tag{21b}$$

In the above we have put $D = \lambda_b/\lambda_a$, the ratio of the dimensionless diffusion coefficients of B and A respectively. The roots are ordered so that,

$$\mathrm{Re}(\omega_+) \geqslant \mathrm{Re}(\omega_-). \tag{22}$$

The next step is to examine the dispersion relation in detail.

2.1. The dispersion relation

The roots of the dispersion relation are readily obtained from (21a) as,

$$\omega_{\pm}(\mu, k_r) = \frac{-p(\mu, k_r) \pm \sqrt{p^2(\mu, k_r) - 4q(\mu, k_r)}}{2}. \tag{23}$$

The local stability of the uniform steady state S is now determined, via (18), by examining the behaviour of $\omega_{\pm}(\mu, k_r)$ in the first quadrant of the (k_r, μ) plane. At any point, (k_r, μ), the functions p and q determine the character of the roots $\omega_{\pm}$. The possibilities can be listed as follows:

(i) $q < 0, \omega_{\pm}$ real with opposite sign. (24a)

(ii) $q > 0, p > 0, q < \frac{1}{4}p^2, \omega_{\pm}$ both real and negative. (24b)

(iii) $q > 0, p > 0, q > \frac{1}{4}p^2, \omega_{\pm}$ complex conjugate with negative real part. (24c)

(iv) $q > 0, p < 0, q < \frac{1}{4}p^2, \omega_{\pm}$ both real and positive. (24d)

(v) $q > 0, p < 0, q > \frac{1}{4}p^2, \omega_{\pm}$ complex conjugate with positive real part. (24e)

In addition, on the boundaries $\omega_{\pm}$ are real and equal when $q = \frac{1}{4}p^2$, form an imaginary pair when $p = 0$, $q > 0$, whilst $\omega_+ = 0$ and $\omega_- = 0$ when $q = 0$ with $p > 0$ and $p < 0$ respectively.

To determine the nature of the regions (i)–(v) in the first quadrant of the (k_r, μ) plane, we consider the loci of the boundary curves,

$$p(\mu, k_r)^2 - 4q(\mu, k_r) = 0, \tag{25a}$$

$$q(\mu, k_r) = 0, \tag{25b}$$

$$p(\mu, k_r) = 0, \quad q(\mu, k_r) > 0. \tag{25c}$$

On substituting from (21a,b) the equations for the curves defined by (25a–c) are given by,

$$k_r^2 = \frac{1}{(D-1)}\left\{\mu^2 \pm 2\sqrt{2}\mu + 1\right\}; \quad \mu, k_r \geqslant 0, \tag{26a}$$

$$\mu^2 = \frac{[1 - Dk_r^2]k_r^2}{[1 + Dk_r^2]}; \quad \mu, k_r \geqslant 0, \tag{26b}$$

$$\mu^2 = 1 - (D+1)k_r^2; \quad \mu \geqslant 0, \quad k_r^2 \leqslant \frac{\sqrt{1+D^2} - 1}{D^2}, \tag{26c}$$

respectively. Henceforth we will refer to the curves defined by (26a–c) as e_E, e_R and e_I respectively. In the quadrant $\mu, k_r \geqslant 0$, e_E, e_R and e_I have only one point of intersection, which is common to all three curves. This point of intersection occurs at (k_r^*, μ_r^*), where,

$$\mu_r^{*2} = 1 - \frac{(D+1)\left[\sqrt{D^2+1} - 1\right]}{D^2}, \quad k_r^{*2} = \frac{\sqrt{D^2+1} - 1}{D^2} \tag{27}$$

At the above point, the curves e_E and e_R intersect tangentially, while e_I intersects both e_E and e_R transversely. The details of the three curves are as follows

(i) e_E

This curve separates regions where $\omega_{\pm}$ are real from where $\omega_{\pm}$ are complex conjugates. Two distinct cases arise for $D \lesseqgtr 1$. With $D < 1$, e_E forms a "semi-loop" attached to the positive μ axis at $\mu = \sqrt{2} \pm 1$, with the stationary point of the loop occuring at $\mu = \sqrt{2}$, $k_r = 1/\sqrt{1-D}$. For $D = 1$, the loop breaks at $k_r = \infty$, with e_E reducing to the pair of straight lines $\mu = \sqrt{2} \pm 1$. With $D > 1$, e_E has three branches. One branch cuts off a triangular

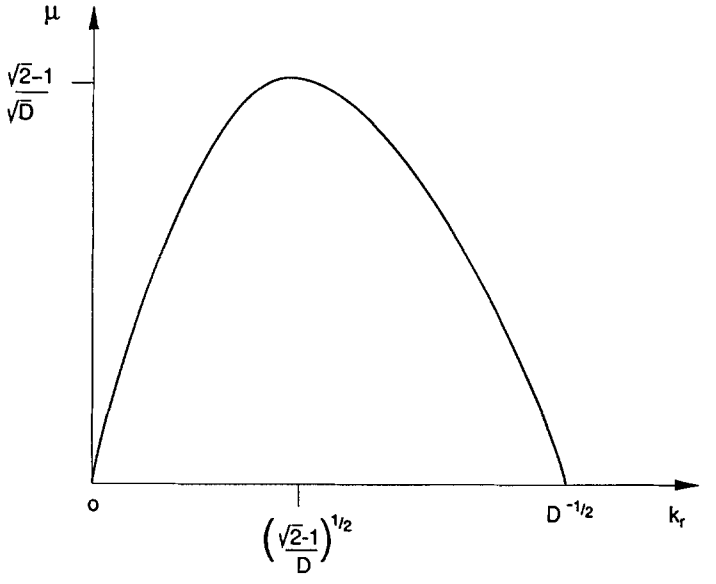

Fig. 1. A sketch of the curve e_R, as defined by equation (26b).

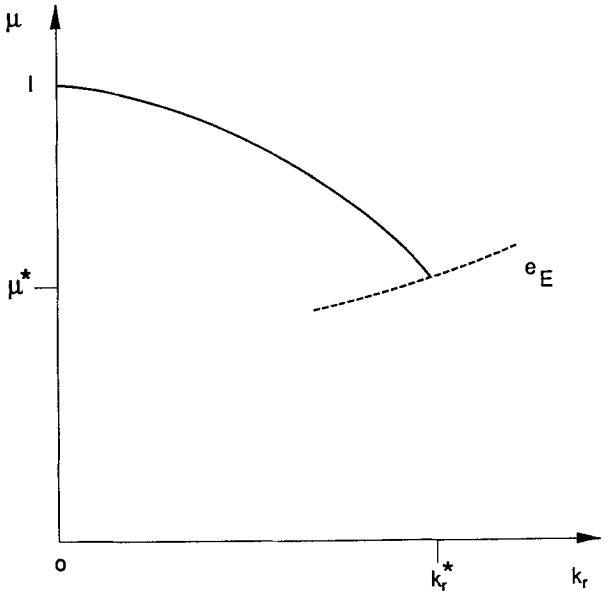

Fig. 2. A sketch of the curve e_I, as defined by equation (26c). μ^* and k_r^* are given by expressions (27).

region in μ, $k_r \geqslant 0$, connecting the point $\mu = \sqrt{2} - 1$, $k_r = 0$ to $\mu = 0$, $k_r = 1/\sqrt{D-1}$. The remaining two branches are monotone increasing with k_r, emanating from the points $\mu = \sqrt{2} + 1$, $k_r = 0$ and $\mu = 0$, $k_r = 1/\sqrt{D-1}$ respectively. Both of these branches have the asymptotic form $\mu \sim \sqrt{D-1}k_r$ as $k_r \to \infty$.

(ii) e_R

On this curve $\omega_+ = 0$. The curve has similar qualitative features for each $D > 0$, having the form of a single hump between the points of $\mu = 0$, $k_r = 0$ and $\mu = 0$, $k_r = 1/\sqrt{D}$. The maximum on the hump occurs at $k_r = \sqrt{(\sqrt{2}-1)/D}$ with $\mu = (\sqrt{2}-1)/\sqrt{D}$. A sketch of e_R in the quadrant k_r, $\mu \geqslant 0$ is shown in Fig. 1.

(iii) e_I

On this curve $\mathrm{Re}(\omega_\pm) = 0$ and is defined only up to intersection with the boundary curve e_E. The form of e_I is qualitatively similar for all $D > 0$. The curve is monotone decreasing for $0 \leqslant k_r \leqslant k_r^*$, with $\mu = 1$ at $k_r = 0$ and $\mu = \mu_r^*$ (< 1) at $k_r = k_r^*$. A sketch of e_I in μ, $k_r \geqslant 0$ is shown in Fig. 2.

2.2. The neutral curve and stability

The conditions required for local stability of the uniform steady state S are most readily obtained by constructing the neutral curve $\mu = \mu_c(k_r)$ in the first quadrant of the (k_r, μ) plane. The neutral curve is the locus of those points for which $\mathrm{Re}(\omega_+) = 0$ and is thus formed from the union of appropriate sections of the curves e_R and e_I. On using (26b,c) we obtain the equation of the neutral curve as,

$$\mu_c^2(k_r) = \begin{cases} 1 - (D+1)k_r^2; & 0 \leqslant k_r \leqslant k_r^* \\ \dfrac{(1 - Dk_r^2)k_r^2}{(1 + Dk_r^2)}; & k_r^* \leqslant k_r \leqslant \dfrac{1}{\sqrt{D}} \end{cases} \tag{28}$$

For each $D > 0$ the neutral curve $\mu_c(k_r)$ connects the point $\mu = 1$, $k_r = 0$ to the point $\mu = 0$, $k_r = 1/\sqrt{D}$, enclosing a bounded region in the lower left hand corner of the positive quadrant in the (k_r, μ) plane.

Qualitative sketches of the neutral curve are shown in Fig. 3 for the differing cases $D \geqslant 1$, $3 - 2\sqrt{2} \leqslant D < 1$, $0 < D < 3 - 2\sqrt{2}$ respectively. Any point above the neutral curve in Fig. 3 has $\mathrm{Re}(\omega_\pm) < 0$ (corresponding to stable behaviour) whilst all points below it have at least $\mathrm{Re}(\omega_\pm) > 0$ (leading to instability).

At a given value of μ, the stability of the uniform steady state S requires $Re[\omega_\pm(\mu, k_r)] < 0$ for each $r = 0, 1, 2, \ldots$, and it is readily deduced from (28) that a necessary and sufficient condition for the local temporal stability of S is provided by

$$\mu > \mu_c^M(D, \lambda_a) = \begin{cases} 1; & D \geqslant 1 \\ \max\{1, \mu_1, \mu_2\}; & 0 < D < 1, \end{cases} \tag{29}$$

where

$$\mu_1^2 = \frac{(1 - N^2\pi^2 D\lambda_a)N^2\pi^2\lambda_a}{(1 + N^2\pi^2 D\lambda_a)},$$

$$\mu_2^2 = \begin{cases} \dfrac{(1 - [N+1]^2\pi^2 D\lambda_a)(N+1)^2\pi^2\lambda_a}{(1 + [N+1]^2\pi^2 D\lambda_a)}; & N \leqslant \dfrac{1}{\pi\sqrt{D\lambda_a}} - 1 \\ 0; \quad \text{otherwise} \end{cases} \tag{30}$$

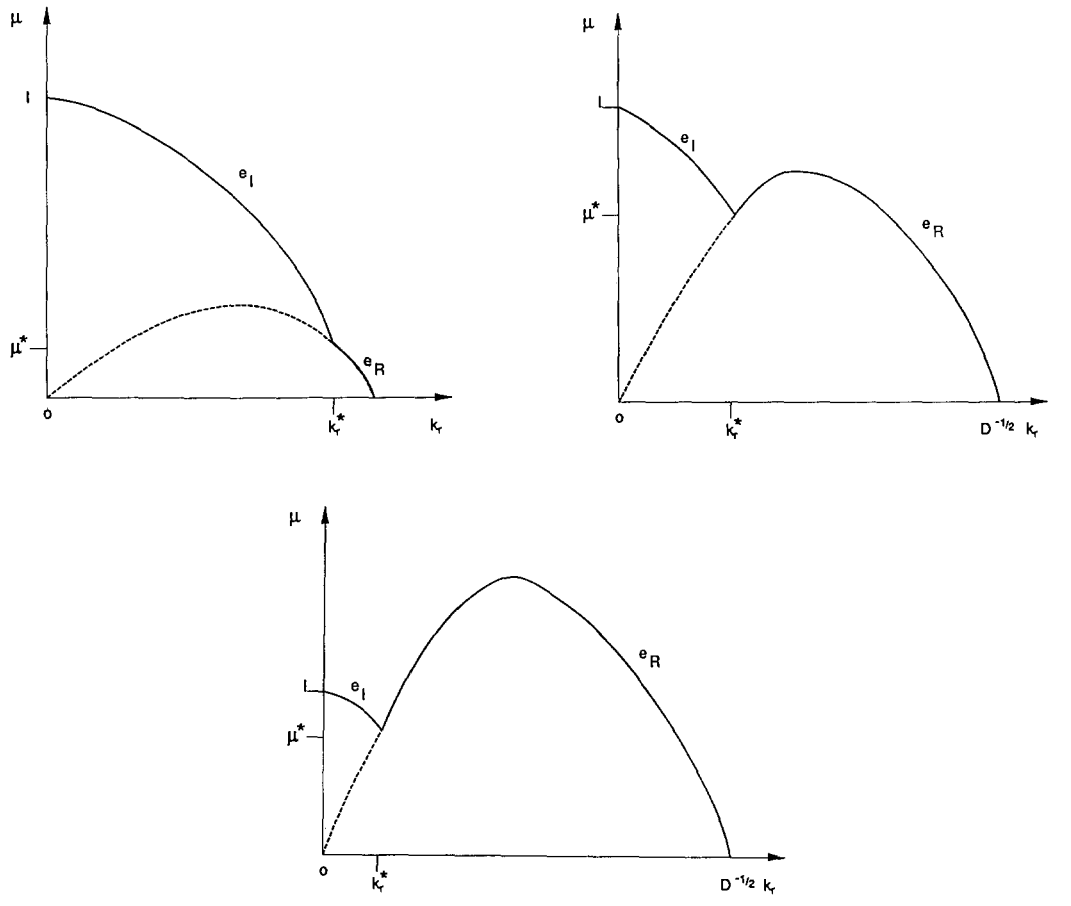

Fig. 3. Sketches of the neutral curves, as given by (28), for (a) $D \geqslant 1$, (b) $3-2\sqrt{2} \leqslant D < 1$, (c) $0 < D < 3-2\sqrt{2}$.

with

$$N = \text{Integer part of } \left\{ \frac{1}{\pi} \sqrt{\frac{\sqrt{2}-1}{D\lambda_a}} \right\}. \tag{31}$$

That is, for each $\mu > \mu_c^M(D, \lambda_a)$, every term in (18) decays exponentially as $t \to \infty$, and any small disturbance imposed upon S will die away. However, for $0 < \mu < \mu_c^M(D, \lambda_a)$, there are terms in (18) which grow exponentially as $t \to \infty$, and the system will diverge from the uniform state S when perturbed.

Before proceeding further, we first examine the nature of $\mu_c^M(D, \lambda_a)$ when $0 < D < 1$. An examination of (28) shows that $\mu_c^M = 1$ when $(3 - 2\sqrt{2}) \leqslant D < 1$. However for $0 < D < (3-2\sqrt{2})$, μ_c^M is monotone increasing with a piecewise linear form and $\mu_c^M \sim (\sqrt{2}-1)/\sqrt{D}$ as $D \to 0$. It is also interesting to consider the limiting forms as $\lambda_a \to 0$ and $\lambda_a \to \infty$. With $\lambda_a \ll 1$ the interval lengths of piecewise linear behaviour decrease, with μ_c^M becoming smooth as $\lambda_a \to 0$; in particular, $\mu_c^M(D, \lambda_a) \sim (\sqrt{2}-1)/\sqrt{D}$ for $0 < D < 3 - 2\sqrt{2}$ as $\lambda_a \to 0$. However, with $\lambda_a \gg 1$, we find that $\mu_c^M = 1$ for $(\sqrt{2}-1)/(\pi^2\lambda_a) < D < 3 - 2\sqrt{2}$ after which μ_c^M increases rapidly and without bound for $0 < D < (\sqrt{2}-1)/(\pi^2\lambda_a)$.

Of particular interest are those values of D and λ_a for which $\mu_c^M > 1$ and Turing instabilities can exist. In this region the effect of diffusion is to destabilize the uniform steady state S and

gives rise to the possible development of locally stable nonuniform steady states (or patterns), as will be demonstrated in the following sections. The above discussion of μ_c^M shows that the existence of Turing instabilities necessarily requires $D < 3-2\sqrt{2}$. Furthermore, for any given D in this range, a Turing instability may be induced by sufficiently decreasing λ_a. Physically this could be achieved by increasing the size of the reacting system or by decreasing the diffusion rates of both reactants A and B, whilst maintaining them at a constant ratio. An examination of (29)–(31) shows that a necessary condition is that

$$\lambda_a \leqslant \frac{\sqrt{2}-1}{\pi^2 D}$$

We now consider the circumstances under which a small amplitude disturbance to the uniform steady state S will evolve into a small, but finite, amplitude spatially and/or temporally periodic state. We identify this type of bifurcation from uniform conditions with pattern formation in the system. Such a bifurcation will be possible only at values of μ for which the uniform steady state S is unstable (otherwise any small amplitude disturbance will decay exponentially with time). Thus we restrict attention to the case where $0 < \mu < \mu_c^M(D, \lambda_a)$.

2.3. Local Bifurcations

The details of determining the nature of local bifurcations from the uniform steady state S follow very closely from Needham and Merkin [19]. As in [19] it is readily shown that small amplitude spatially and/or temporally periodic states bifurcate out of S at those values of μ for which one of the curves k_r = constant ($r = 0, 1, 2, \ldots$) intersects either of the curves e_R or e_I, i.e. at those values of μ for which a neutral mode exists in the linearized theory. Thus, the linearized theory of the previous section enables us to identify the bifurcation points in $0 < \mu < \mu_c^M$. The local behaviour of a particular bifurcation can then be obtained by developing a weakly nonlinear theory.

For a bifurcation occuring at $\mu = \mu_b$ with corresponding wave number k_b, (for some positive integer b), the details may be summarized as follows:

(i) For (k_b, μ_b) on e_I there is a Hopf bifurcation, leading to the appearance of a small amplitude spatially and temporally periodic solution when $0 < |\mu_b - \mu| \ll 1$, with amplitude of $O(|\mu_b - \mu|^{1/2})$ and spatial wave length $2/b$.

(ii) For (k_b, μ_b) on e_R there is a pitchfork bifurcation leading to the appearance of two small spatially periodic patterns when $0 < |\mu - \mu_b| \ll 1$. These are related through reflectional symmetry and have amplitude of $O(|\mu - \mu_b|^{1/2})$ and spatial wavelength $2/b$.

By definition the first bifurcation occurs at $\mu = \mu_c^M$, when $k_r = k_r^M$, corresponding to the integer r^M where, from (29–31) we have

$$r^M = \begin{cases} 0; & D > 3-2\sqrt{2} \\ N; & D \leqslant 3-2\sqrt{2}, \quad \mu_1 > \mu_2 \\ N+1; & D \leqslant 3-2\sqrt{2}, \quad \mu_1 < \mu_2 \end{cases} \tag{32}$$

At this bifurcation point all other wave numbers k_r, $r \neq r^M$ have $\mathrm{Re}[\omega_\pm(\mu_c^M, k_r)] < 0$, and we deduce that the resulting bifurcated pattern is locally and absolutely stable, at least for $0 < |\mu_c^M - \mu| \ll 1$. However, each subsequent bifurcation at $\mu = \mu_b < \mu_c^M$ will lead to a pattern that is at most partially stable when $0 < |\mu_b - \mu| \ll 1$. That is, the pattern is temporally stable to perturbations composed of all but a finite number of wave numbers k_r. In particular,

the set of wave numbers to which the bifurcating pattern is unstable, are exactly those wave numbers k_r associated with bifurcations at larger values of μ. In this case the extension of bifurcating branches will lead to multiple patterned states for each $0 < \mu < \mu_c^M$. At any fixed $\mu < \mu_c^M$, the number of available patterned states which are locally and absolutely stable will clearly depend upon how the bifurcating branches behave and interact globally (i.e. away from the weak nonlinear limit $0 < |\mu_b - \mu| \ll 1$) to induce changes of local stability and associated secondary bifurcations. However, before considering the global nature of the branches, we first complete the details of the local bifurcations. An important point to note is that the bifurcation at $\mu = \mu_c^M$ has either $k_{rM} = 0$ and lies on e_I or has $k_{rM} > 0$ and lies on e_R. Thus the only pattern which can be locally and absolutely stable at bifurcation is either spatially homogeneous and temporally periodic (a trivial pattern) or a steady spatially periodic pattern.

We can also obtain information about the number of local bifurcations occuring in $\mu \leqslant \mu_c^M$. It is readily shown, from (28), that for any fixed D, when $\lambda_a \geqslant 1/\pi^2 D$, the only local bifurcation in $\mu \leqslant \mu_c^M$ is that at $\mu = \mu_c^M = 1$, which has corresponding $k_{rM} = 0$ (via (29)–(31)). This leads to the spatially homogeneous, stable, temporally periodic state in $0 < 1 - \mu \ll 1$. In this case we would expect only trivial pattern formation in $0 < \mu < 1$, as no further local bifurcation branches appear as μ decreases from unity. However, for $\lambda_a < 1/(\pi^2 D)$ the total number of local bifurcations in $\mu \leqslant \mu_c^M$ is given by,

$$N_b = R_1 + R_2 + 1, \tag{33}$$

where,

$$\begin{aligned} R_1 &= \text{Integer part of} \left\{ \frac{\sqrt{\sqrt{D^2+1}-1}}{\pi\sqrt{\lambda_a D}} \right\}, \\ R_2 &= \text{Integer part of} \left\{ \frac{1}{\pi\sqrt{\lambda_a}\sqrt{D}} \right\}. \end{aligned} \tag{34}$$

A total of $[R_1 + 1]$ of these are Hopf bifurcations from the curve e_I, and therefore have $\mu^* \leqslant \mu_b \leqslant 1$. The remaining R_2 are pitchfork bifurcations from the curve e_R, and have $0 < \mu_b \leqslant (\sqrt{2} - 1)/\sqrt{D}$. We label these bifurcation points as $\mu_b^{(i)}$ $(i = 1, 2, \ldots, N_b)$, with $\mu_c^M = \mu_b^{(1)} > \mu_b^{(2)} > \cdots > \mu_b^{(N_b)}$, with the corresponding pattern denoted by P^i. A lower bound on the spatial wavelength associated with these patterns at bifurcation is given by $2/R_2$ for the steady periodic patterns and $2/R_1$ for the spatially and temporally periodic patterns.

As noted earlier, the only pattern which is locally, absolutely, stable at bifurcation is that which emerges from the steady state S at μ_c^M, with the remaining patterns being only partially stable at their bifurcation. Thus, with decreasing μ, we are able to deduce that the system will behave in the following way when it is disturbed from the uniform steady state S with an arbitrary small, perturbation:

(i) $\mu \geqslant \mu_c^M$

The uniform steady state S is locally absolutely stable, and the disturbance decays away exponentially as $t \to \infty$, with the system returning to S.

(ii) $\mu_b^{(2)} \geqslant \mu < \mu_c^M$

The uniform steady state S is unstable to the single mode with wave number k_{rM}, which has exchanged stability with the locally, absolutely stable pattern created in $\mu < \mu_c^M$ through the local bifurcation at $\mu = \mu_c^M$. Thus, the uniform steady state S develops into the pattern P^1 as $t \to \infty$.

(iii) $0 < \mu < \mu_b^{(2)}$

As μ decreases below $\mu_b^{(2)}$, the uniform steady state S becomes unstable to an increasing number of modes with wave number k_{r_1}, $k_{r_2}, \ldots$, as μ decreases through the successive bifurcation values $\mu_b^{(2)}$, $\mu_b^{(3)}, \ldots$, whilst an increasing number of possible patterned states P^2, $P^3, \ldots$, are becoming available on the bifurcation branches. These may achieve local, absolute, stability via secondary bifurcations, and provide potential candidates into which the system may develop as $t \to \infty$.

We now consider further case (ii), when $\mu_b^{(2)} < \mu < \mu_c^M$. There are two situations to discuss:

(iia) $D \geqslant 3 - 2\sqrt{2}$

With $D \geqslant 3 - 2\sqrt{2} = 0.171573$, we have $\mu_c^M = 1$ and $k_{rM} = 0$, via (29)–(31). Thus the stable pattern to which the system develops is the spatially, homogeneous temporally oscillating state (which is the limit cycle state L of the well-stirred system). We conclude that in this case no non-trivial patterns can persist at small amplitude. Stable pattern formation, if it occurs at all, must be associated with stabilization at lower values of μ, on the global extensions of the local bifurcation branches discussed in this section.

(iib) $D < 3 - 2\sqrt{2}$

For $D < 3 - 2\sqrt{2}$ and $\lambda_a > (\sqrt{2} - 1)/(\pi^2 D)$ the situation is as described above. However, with $\lambda_a \leqslant (\sqrt{2} - 1)/(\pi^2 D)$, Turing instability is possible. That is, we can have $\mu_c^M > 1$ and $k_{rM} > 0$. In this case the local bifurcation at $\mu = \mu_c^M$ leads to a stable, nontrivial, steady, periodic pattern to which the system will develop as $t \to \infty$. The wavelength of this pattern, when $0 < |\mu_c^M - \mu| \ll 1$ is $2/r^M$, with amplitude of $O(|\mu_c^M - \mu|^{1/2})$. This pattern will persist for each $\mu_b^{(2)} < \mu < \mu_c^M$.

The above predictions have been made on the basis of a linear stability analysis of the spatially uniform steady state S. To determine the state to which the system will evolve when S is temporally unstable the full nonlinear equations must be considered. We start by considering the solution near the pitchfork bifurcations identified above by developing a weakly nonlinear theory.

3. Non-local pattern formation

In the previous section we have shown that, in order for the system to bifurcate locally to a stable, non-homogeneous, steady state (pattern), we must have $\mu_c^M > 1$ (where μ_c^M is defined by (29)). This, in turn, gives a necessary condition for the local bifurcation to stable pattern forms that

$$D < 3 - 2\sqrt{2} \tag{35a}$$

For the rest of our discussion we limit attention to values of D which satisfy condition (35a). Also, with condition (35a) satisfied the bifurcating solutions with wave number $k_r = r\pi\sqrt{\lambda_a} > 0$ correspond to a value μ_b where

$$\mu_b^2 = \frac{(1 - Dk_r^2)k_r^2}{1 + Dk_r^2} \tag{35b}$$

Note that a direct consequence of (35b) is that we require $Dk_r^2 < 1$. We start our discussion of the nature of the spatially non-homogeneous solution branches with a weakly nonlinear analysis, *i.e.* we develop a solution on the assumption that $|\mu - \mu_b| \ll 1$.

3.1. Weakly nonlinear theory

We begin our discussion by putting

$$\mu = \mu_b - \gamma\epsilon^2, \quad 0 < \epsilon \ll 1 \tag{36}$$

where μ_b is given by (35b) and where $\gamma = \pm 1$, depending on whether the pattern form bifurcates initially into $\mu < \mu_b$ ($\gamma = 1$) or μ_b ($\gamma = -1$). We then proceed with the solution, as in Needham and Merkin [19], by looking for a solution by expanding about stationary state S in powers of ϵ. We find that the cubic nonlinearity generates an inhomogeneous forcing term at $O(\epsilon^3)$ formed from the fundamental neutral mode. This, in turn, leads to secular terms, which are of $O(\epsilon^3 t)$. To overcome this problem and to obtain a uniform expansion we use the method of multiple scales, [20], in which we introduce the slow time variable $\tau = \epsilon t$. Consequently, we first put

$$a(x,t,\tau) = \mu^{-1} + u(x,t,\tau), \quad b(x,t,\tau) = \mu + v(x,t,\tau) \tag{37}$$

and look for a solution of the resulting equations for u and v by expanding in powers of ϵ of the form

$$\begin{aligned} u &= u_1\epsilon + u_2\epsilon^2 + u_3\epsilon^3 + \cdots \\ v &= v_1\epsilon + v_2\epsilon^2 + v_3\epsilon^3 + \cdots \end{aligned} \tag{38}$$

where the coefficients u_i, v_i are all functions of x and the two time variables t and τ. The leading order terms satisfy the linear homogeneous problem (16), with μ replaced by μ_b. The solution of these equations can be solved in terms of Fourier series with all wave numbers present. However, it is only a particular wave number k_r (with μ_b given by (35a)) which gives a neutral mode. Consequently, the solution approaches this mode as $t \to \infty$, and the solution we require at this stage is then

$$\begin{pmatrix} u_1 \\ v_1 \end{pmatrix} = A(\tau) \begin{pmatrix} d_1 \\ d_2 \end{pmatrix} \cos(r\pi x) \tag{39a}$$

where A is, as yet, an undetermined amplitude and where

$$\frac{d_1}{d_2} = -\frac{1 + Dk_r^2}{k_r^2} \tag{39b}$$

At $O(\epsilon^2)$ we obtain a linear inhomogeneous problem. The equations are the same as at the previous stage but now involve quadratic forcing terms resulting from the nonlinear interaction

of the leading order terms. We require only the solution of this system in the limit as $t \to \infty$, finding after some calculation, that

$$\begin{pmatrix} u_2 \\ v_2 \end{pmatrix} = \frac{A^2 E}{2\mu_b^2} \begin{pmatrix} -1 \\ 0 \end{pmatrix} + \frac{A^2 E}{2\Delta} \begin{pmatrix} -1 - 4Dk_r^2 \\ 4k_r^2 \end{pmatrix} \cos(2r\pi x) + B \begin{pmatrix} d_1 \\ d_2 \end{pmatrix} \cos r\pi x \tag{40a}$$

where B is a further function of the slow time τ and where

$$E = 2\mu_b\, d_1\, d_2 + \mathrm{d}_2^2/\mu_b, \quad \Delta = 2\mu_b^2 - (4k_r^2 + \mu_b^2)(1 - 4Dk_r^2) \tag{40b}$$

At $O(\epsilon^3)$ we again have a linear inhomogeneous problem with the same left hand sides as before, but now with right hand side forcing terms which arise from the nonlinear interaction of the previous terms in the expansions. When we come to consider the nature of the solution of this system as $t \to \infty$ we find that secular terms arise. These have essentially three sources; the interaction of solutions (39a, 40a), the form for μ given by (36), and differentiation with respect to the slow time variable τ. Following the method of multiple scales, we equate these terms to zero which, in turn, leads to an equation for the amplitude function $A(\tau)$. We found that the most straightforward way to proceed was to follow Auchmuty and Nicolis [21] and apply the solvability criteria for the linear operator, given essentially by equations (16), with known forcing terms at both $O(\epsilon)$ and $O(\epsilon^3)$. We found, after a somewhat lengthy calculation, $A(\tau)$ to be given by the equation

$$\frac{\mathrm{d}A}{\mathrm{d}\tau} = -CGA\left(A^2 - \frac{\mu_b}{G\gamma}\right) \tag{41a}$$

where C is a constant, positive for all parameter values, and where

$$\frac{G}{d_2^2} = \frac{28\theta^3 + 75\theta^2 - 24\theta + 1}{24(1-\theta)(4\theta^2 + 5\theta - 1)}, \quad \theta = Dk_r^2 = \lambda_a D r^2 \pi^2 \tag{41b}$$

with expression (28) requiring $\theta < 1$. Consider equation (41a). If $G > 0$ we take $\gamma = 1$ so that the bifurcation pattern form appears, initially at least, in $\mu < \mu_b$. A further consideration of equation (41a) shows that this solution is stable, with

$$A \to A_s = \pm\left(\frac{\mu_b}{G}\right)^{1/2} \quad \text{as } \tau \to \infty \tag{42}$$

Alternatively, if $G < 0$, we take $\gamma = -1$, so that the bifurcated pattern form appears initially in $\mu > \mu_b$ but now the non-trivial steady states

$$A_s = \pm\left(\frac{\mu_b}{|G|}\right)^{1/2}$$

of equation (41a) are unstable.

This leads us naturally to consider the function $G = G(\theta)$ for $0 < \theta < 1$. It is straightforward to show that G has two positive zeros (at $\theta_1 = 0.049449$, $\theta_2 = 0.243089$) and that the denominator is zero at $\theta_3 = (\sqrt{41} - 5)/8 = 0.175391$ and at $\theta = 1$. Thus for $0 < \theta < \theta_1$, $G < 0$, for $\theta_1 < \theta < \theta_3$, $G > 0$, ($|G| \to \infty$ as $\theta \to \theta_3$), for $\theta_3 < \theta < \theta_2$, $G < 0$ and for $\theta_2 < \theta < 1$, $G > 0$.

We now examine the consequence of the above discussion on G for the possible pattern formation as the dimensionless parameters μ, D and λ_a of the system are varied. Suppose

these parameters are such that only the first mode ($r = 1$) can grow with all the other modes ($r = 2, 3, \ldots$) being stable. This requires $k_1 < D^{-1/2}$ and $k_r > D^{-1/2}$ for all $r > 1$, (Fig. 3c), giving the condition

$$\frac{1}{4} < \lambda_a D\pi^2 < 1 \tag{43a}$$

Thus $\theta > \theta_2$ and the only possibility is for $G > 0$. Furthermore, we require $\mu_{b,1} > 1$, so that the homogeneous stationary state S is stable. This leads to the extra condition that $\lambda_a \pi^2$ should lie in the interval

$$\frac{1 - D - \sqrt{1 - 6D + D^2}}{2D} < \lambda_a \pi^2 < 1 \frac{1 - D + \sqrt{1 - 6D + D^2}}{2D}, \quad D < 3 - 2\sqrt{2} \tag{43b}$$

Here we are using the notation $\mu_{b,r}$ to refer to the value of μ at the bifurcation corresponding to wave number k_r. Hence, in this case the bifurcation is always supercritical (stable). If we characterize the solution branches by giving $b(0)$ the value of b on $x = 0$, we have, from (39a) and (42) that

$$b(0) = \mu_b \pm \left(\frac{\mu_b}{G}\right)^{1/2} (\mu_b - \mu)^{1/2} + \cdots \tag{43c}$$

close to the bifurcation point at $\mu = \mu_b$.

Next consider the case when the dimensionless parameters are such that the first two modes ($r = 1, r = 2$) can grow, with all the higher modes being stable, *i.e.* we have $k_1 < k_2 < D^{-1/2}$, giving the condition

$$\frac{1}{9} < \lambda_a D\pi^2 < \frac{1}{4} \tag{44a}$$

Thus θ can now be in one of the ranges $\theta_1 < \theta < \theta_3$ ($G > 0$), $\theta_3 < \theta < \theta_2$ ($G < 0$) or $\theta_2 < \theta < \frac{1}{4}$ ($G > 0$). Also, we have that

$$\begin{aligned} &\mu_{b,2} > \mu_{b,1} \quad \text{when} \quad \theta < \theta_3 \\ &\mu_{b,1} > \mu_{b,2} \quad \text{when} \quad \theta > \theta_3 \end{aligned} \tag{44b}$$

Thus there are three possibilities as the bifurcation parameter μ is decreased. Pattern forms can bifurcate from the homogeneous stationary state S first at either $\mu = \mu_{b,1}$ (if $\lambda_a D\pi^2 > \theta_3$) or at $\mu = \mu_{b,2}$ (if $\lambda_a D\pi^2 < \theta_3$). In the former case the bifurcation can be either supercritical or subcritical (unstable). Whereas in the latter case it is always supercritical. This discussion can be continued in an obvious way and the bifurcations characterized as increasing numbers of modes become unstable. We note that when $\lambda_a D\pi^2 = \theta_3 = (\sqrt{41} - 5)/8$, $\mu_{b,1} = \mu_{b,2}$ and the bifurcation becomes degenerate. We next examine this aspect in more detail along the lines suggested by Schaeffer and Golubitsky [22] and Bauer *et al.* [23].

3.2. Solution near the degeneracy

From (35b) we can see, for a given value of D, that, when $\lambda_a = \lambda_0 = (\sqrt{41} - 5)/(8\pi^2 D) = 0.01777/D$, the bifurcations with wave numbers k_1 and k_2 occur at the same value of $\mu = \mu_0 = (\sqrt{41} - 5)/(4D^{1/2}) = 0.3508 D^{-1/2}$, (for $\mu > 1$ we require $D < \frac{1}{8}(33 - 5\sqrt{41}) = 0.1230$).

To obtain a solution near this degeneracy (double zero eigenvalue of the linear system (16)), we first write

$$\lambda = \lambda_0 + \gamma\delta, \qquad 0 < \delta \ll 1 \tag{45a}$$

where $\gamma = \pm 1$ as before. We then apply transformation (37) and look for a solution by expanding

$$\mu = \mu_0 + \bar{\mu}_1\delta + \bar{\mu}_2\delta^2 + \cdots$$

$$\begin{pmatrix} u \\ v \end{pmatrix} = \begin{pmatrix} u_1 \\ v_1 \end{pmatrix}\delta + \begin{pmatrix} u_2 \\ v_2 \end{pmatrix}\delta^2 + \begin{pmatrix} u_3 \\ v_3 \end{pmatrix}\delta^3 + \cdots \tag{45b}$$

and concentrate at this stage on obtaining the steady state solutions.

At $O(\delta)$ we obtain the linear homogeneous system (16) with μ replaced by μ_0 (and the time derivates put to zero). This system has the non-trivial solution

$$\begin{pmatrix} u_1 \\ v_1 \end{pmatrix} = A_1 \begin{pmatrix} d_1(1) \\ d_2(1) \end{pmatrix} \cos \pi x + A_2 \begin{pmatrix} d_1(2) \\ d_2(2) \end{pmatrix} \cos 2\pi x \tag{46}$$

where $(\mathrm{d}_1(j))/(\mathrm{d}_2(j)) = -2/(\lambda_0 j^2\pi^2 + \mu_0^2)$. To determine the amplitudes A_1 and A_2 we need to consider the equations at $O(\delta^2)$. Here we again obtain the linear system (16) but now with forcing terms on the right hand side involving resonant terms in $\cos \pi x$ and $\cos 2\pi x$. We then invoke the Fredholm alternative to provide a solvability condition for these equations, which, after some calculation, results in equations for A_1 and A_2 in the form

$$A_1(-R_1\gamma + R_2\bar{\mu}_1 + R_3A_2) = 0 \tag{47a}$$

$$A_2(P_1\gamma + P_2\bar{\mu}_1) + P_3A_1^2 = 0 \tag{47b}$$

where the constants R_i, P_i $(i = 1, 2, 3)$ are given by

$$R_1 = -\frac{1}{2}\pi^2(f_1(1)\, d_1(1) + D\, d_2(1) f_2(1)),$$

$$R_2 = (f_1(1) - f_2(1))\mu_0\, d_1(1),$$

$$R_3 = \frac{1}{4}(f_1(1) - f_2(1))Q_2, \text{ with}$$

$$Q_2 = 2\mu_0(d_1(1)\, d_2(2) + d_2(1)\, d_1(2)) + \frac{2}{\mu_0}\, d_2(1)\, d_2(2)$$

and $P_1 = 2\pi^2(d_1(2)f_1(2) + D\, d_2(2)f_2(2))$,

$$P_2 = (f_1(2) - f_2(2))\mu_0 d_1(2),$$

$$P_3 = \frac{1}{4}(f_1(2) - f_2(2))Q_1 \text{ with}$$

$$Q_1 = 2\mu_0\, \mathrm{d}_1(1)\, d_2(1) + d_2(1)^2/\mu_0 \text{ and}$$

$$\frac{f_2(j)}{f_1(j)} = \frac{\lambda_0 j^2\pi^2 + \mu_0^2}{\mu_0^2}.$$

To proceed, we need to determine the signs of coefficients in equations (47). We find, again after a little calculation, that

$$R_1 > 0, \quad R_2 > 0, \quad P_1 > 0, \quad P_2 > 0 \quad \text{and} \quad R_3P_3 > 0 \tag{48}$$

We can now determine the solutions of equations (47) (using (48)) in terms of the parameter $\bar{\mu}_1$ as

$$A_1 = A_2 = 0 \text{ for all } \bar{\mu}_1 \tag{49a}$$

$$A_1 = 0, \quad A_2 \text{ arbitrary at } \bar{\mu}_1 = -\frac{P_1\gamma}{P_2} \tag{49b}$$

$$A_2 = \frac{\gamma R_1 - R_2\bar{\mu}_1}{R_3}, \quad A_1 = \pm\left(\frac{(\gamma P_1 + P_2\bar{\mu}_1)(\bar{\mu}_1 R_2 - \gamma R_1}{P_3R_3}\right)^{1/2} \tag{49c}$$

This latter solution (49c) for A_1 occurs in $\bar{\mu}_1 > (R_1/R_2)$ and $\bar{\mu}_1 - (P_1/P_2)$ for $\gamma = 1$ (*i.e.* $\lambda > \lambda_0$) or in $\bar{\mu}_1 < -(R_1/R_2)$ and $\bar{\mu}_1 > (P_1/P_2)$ for $\gamma = -1$ (*i.e.* $\lambda < \lambda_0$).

To resolve the arbitrariness in solution (49b) at $\bar{\mu} = \bar{\mu}_1^* = 2\pi^2\gamma(\sqrt{41}-3)/(16\mu_0)$ we need to consider the terms of $O(\delta^3)$. To do this we add into our solution at $O(\delta^2)$, the complementary functions

$$B_1\begin{pmatrix} d_1(1) \\ d_2(1) \end{pmatrix}\cos\pi x + B_2\begin{pmatrix} d_1(2) \\ d_2(2) \end{pmatrix}\cos 2\pi x \tag{50}$$

Then, since the equations are still linear, given by (16), with further resonant terms on their right hand sides, we again invoke the Fredholm alternative to obtain a solvability condition. This leads to equations in the form

$$B_1(S_1 + A_2S_2) = 0 \tag{51a}$$

$$B_2S_3 + S_4A_2 + S_5A_2^3 = 0 \tag{51b}$$

for certain constants S_i $(i = 1, \ldots, 5)$. Equations (51) have the required solution $B_1 = B_2 = 0$ provided $A_2^2 = -(S_4/S_5)$. This determines A_2 at $\bar{\mu}_1 = \bar{\mu}_1^*$ as

$$A_2^2 = -\frac{1}{d_2(2)^2G_2}\left(\frac{\pi^2}{\lambda_0}\left(\frac{7\sqrt{41}+101}{128}\right) + \bar{\mu}_1^{*2} + \mu_0\bar{\mu}_2\right) \tag{52}$$

where G_2 is the value of G given by expression (41b) evaluated at $\theta = Dk_2^2 = 4\lambda_a D\pi^2$. A simple calculation gives $G_2 = 7\sqrt{41}(\sqrt{41}+9)/720 > 0$. It is clear then that the existence of A_2 given by equation (52) requires $\bar{\mu}_2 < 0$.

To determine the stability of the solutions given above we can either introduce a long time scale $T = \delta t$ and use the method of multiple scales in the full time-dependent system, or we can linearize these equations about the appropriate steady states. In either case, we find that the stability is governed by the eigenvalues of the Jacobian

$$J = \begin{pmatrix} \gamma R_1 - \bar{\mu}_1 R_2 - R_3A_2 & -R_3A_1 \\ -2P_3A_1 & -P_1\gamma - P_2\bar{\mu}_1 \end{pmatrix} \tag{53}$$

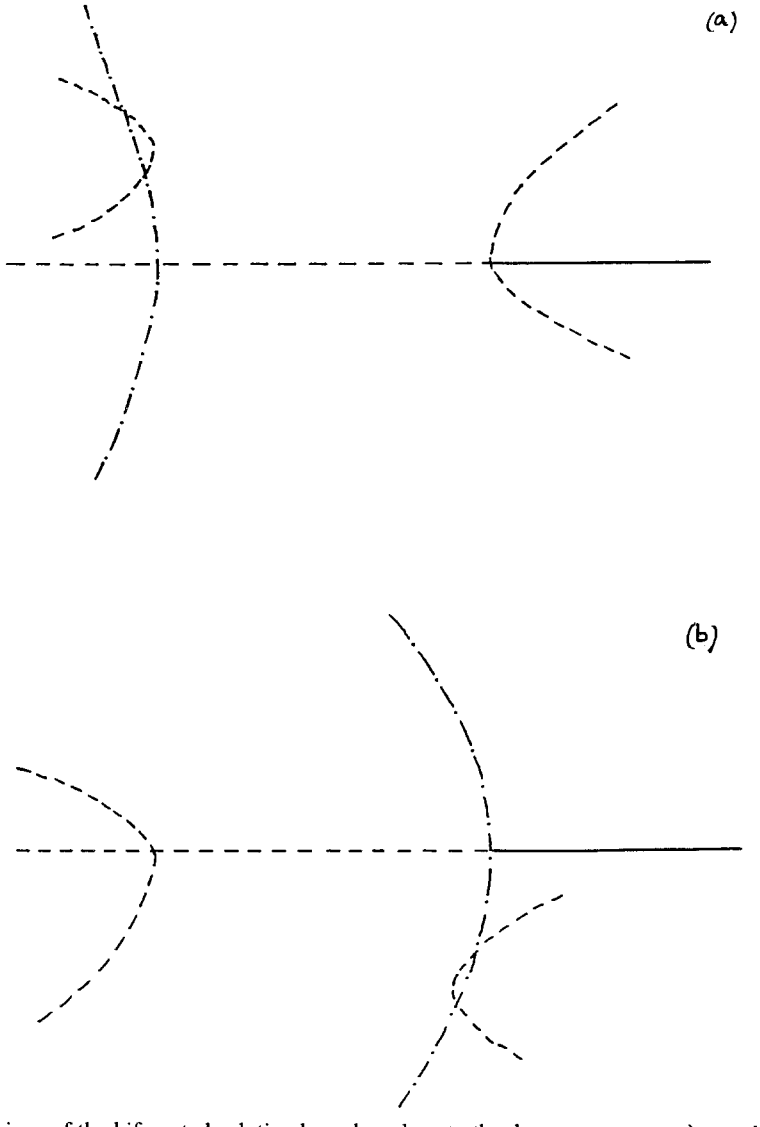

Fig. 4. The behaviour of the bifurcated solution branches close to the degeneracy at μ_0, λ_0 as obtained from the weakly nonlinear analysis, (a) $\lambda > \lambda_0$ (b) $\lambda < \lambda_0$. Here sketches of $b(0) - \mu_0$ against $\bar{\mu} = \mu - \mu_0$ are shown.

From (48) we can see that the steady state (49a) is: stable for $\bar{\mu}_1 > (R_1/R_2)$ and unstable otherwise when $\gamma = 1$, stable for $\bar{\mu} > (P_1/P_2)$ unstable otherwise for $\gamma = -1$. For steady state (49c) the eigenvalues of J are

$$\lambda^{\pm} = \frac{1}{2}\left(-(P_1\gamma + P_2\bar{\mu}_1) \pm \sqrt{(P_1\gamma + P_2\bar{\mu}_1)^2 + 8P_3R_3A_1^2}\right) \tag{54}$$

From (54) it follows that this steady state is unstable for all parameter values for which it exists (an $\gamma = \pm 1$). The stability of the steady state (49b) is indeterminate at this stage, (53) leads to a double zero-eigenvalue and a consideration of the higher order terms is required.

The behaviour of the solution close to $\mu = \mu_0$ is illustrated in Fig. 4 where we sketch $A_1 + (d_2(2))/(d_2(1))A_2 (\simeq b(0) - \mu_0)$ against μ for the two cases $\gamma = 1$ $(\lambda > \lambda_0)$ and

$\gamma = -1$ ($\lambda < \lambda_0$). We now leave the weakly nonlinear theory and examine the nature of the pattern forms away from their bifurcation points.

3.3. NUMERICAL METHOD

To follow the pattern forms away from their bifurcation points we used the spectral method, see, for example, Canato *et al.* [24], to reduce the pair of partial differential equations (14a,b) to a system of coupled ordinary differential equations. Thus we approximated the exact solution by finite expansions for the functions $a(x,t), b(x,t)$ in terms of the appropriate eigenfunctions of the Laplacian operator in (14a,b) and boundary conditions (14c) on the interval $[0,1]$, *i.e.* we took

$$a(x,t) = \sum_{r=0}^{N} a_r(t)\cos(r\pi x), \quad b(x,t) = \sum_{r=0}^{N} b_r(t)\cos(r\pi x) \tag{55}$$

The residual function, obtained when expressions (55) are substituted into equations (14a,b), is then chosen so as to be orthogonal to each of the eigenfunctions $\cos(r\pi x)$, $(r = 0, 1, 2, \cdots, N)$. This leads to a system of $2(N+1)$ ordinary differential equations for the $a_r(t)$, $b_r(t)$ which, because of the relative simplicity of the cubic nonlinearity, could be easily generated. The solutions were then followed numerically using the path following package PATH, Kaas-Petersen [25]. This procedure also calculated the temporal eigenvalues at each point and thus the stability of the solution could also be determined.

The major advantage of using the spectral method over the use of finite differences or the pseudo-spectral method [26] is that a relatively small number of terms in expansions (55) are required to generate comparatively accurate solutions, and consequently large savings in computational time can be achieved. We found this to be the case for the present problem. We compared results obtained with $N = 5$ and $N = 10$ and found them to be in very good agreement (better than graphical accuracy). In the results described below we use the value of $b(x,t)$ on $x = 0$ (labelling this $b(0)$) to characterize the solution branches and use μ as the bifurcation parameter.

3.4. NUMERICAL RESULTS

From the weakly nonlinear theory we have been able to identify various cases that can arise. Consider first the case when only one non-zero wave number k_1 becomes unstable. We have seen here that the only possibility is for a supercritical pitchfork bifurcation, initially in $\mu < \mu_{b,1}$. The bifurcated solution branches (patterns) obtained numerically by the method described above are shown in Fig. 5. Here we chose $D = 0.01$ and $\lambda_a \pi^2 = 42.25$, giving $\mu_{b,1} = 4.142$. Figure 5 shows that the stable pattern that emerges at $\mu_{b,1}$ into $\mu < \mu_{b,1}$ continues throughout in this region, remaining stable until it undergoes a supercritical Hopf bifurcation at $\mu = \mu_{H,1} = 0.87995$. For $\mu < \mu_{H,1}$ the non-homogeneous steady solution is unstable. The Hopf bifurcation at $\mu = \mu_{H,1}$ gives rise to stable, temporally periodic, spatially non-uniform behaviour in $\mu < \mu_{H,1}$ (these solution branches are not shown in Figure 5). This aspect will be discussed in more detail below.

Next consider the case when the two modes with wave numbers k_1 and k_2 become unstable. Here we have seen that there are three cases to consider, namely $\mu_{b,1} > \mu_{b,2}$ with the pitchfork bifurcation at $\mu = \mu_{b,1}$ being supercritical, $\mu_{b,1} > \mu_{b,2}$ with the pitchfork bifurcation at $\mu = \mu_{b,1}$ being subcritical and $\mu_{b,2} > \mu_{b,1}$ with the pitchfork bifurcation at $\mu = \mu_{b,2}$

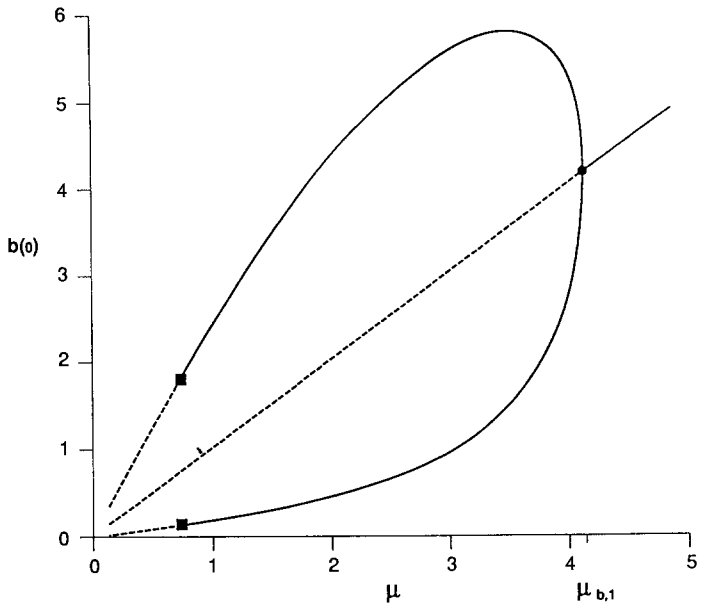

Fig. 5. Bifurcation diagram (a plot of $b(0)$ against μ) for $D = 0.01$, $\lambda_a \pi^2 = 42.25$ when only the first mode k_1 becomes unstable. Here — represents a stable solution, – – – an unstable solution, ● a supercritical pitchfork bifurcation, ○ a subcritical pitchfork bifurcation and ■ a supercritical Hopf bifurcation.

supercritical. These three cases are shown in Figs. 6. The first case is illustrated in Fig. 6a, where we have taken $D = 0.01$, $\lambda_1 \pi^2 = 24.4$, giving $\mu_{b,1} = 3.8506$, $\mu_{b,2} = 1.0888$. Here the picture is similar to the previous case. The stable pattern generated at $\mu = \mu_{b,1}$ remains stable in $\mu < \mu_{b,1}$ until it undergoes a supercritical Hopf bifurcation. The non-homogeneous steady solution bifurcating from S at $\mu = \mu_{b,2}$ does not interact with this stable pattern.

Next consider the second possibility. This is illustrated in Fig. 6b, where we have taken $D = 0.01$, $\lambda_a \pi^2 = 20.0$, with then $\mu_{b,1} = 3.6515$ $\mu_{b,2} = 2.9814$. The picture is similar to the previous case, with the stability of the pattern being lost via a Hopf bifurcation. The main difference is that now the spatially non-homogeneous solution that emerges at $\mu = \mu_{b,1}$ is initially unstable and does so into $\mu > \mu_{b,1}$. There then follows a saddle-node bifurcation which stabilizes the solution producing a stable pattern as before.

Finally, consider the third possibility. This is illustrated in Figure 6c where we have taken $D = 0.1$, $\lambda_a \pi^2 = 1.4$, with the $\mu_{b,1} = 1.0277$ $\mu_{b,2} = 1.2568$. In this case the bifurcation diagram is more complicated. The primary bifurcation is now at $\mu = \mu_{b,2}$ producing stable patterns in $\mu < \mu_{b,2}$. These lose stability, again through supercritical Hopf bifurcations. Now a secondary loop of solutions is seen which remains unstable throughout, this branch can be thought of as either emerging from the pitchfork bifurcation from the homogeneous solution at $\mu = \mu_{b,1}$ or as emerging from a pitchfork bifurcation from the original bifurcated solution branch emerging at $\mu = \mu_{b,2}$ after this branch has gone unstable at the Hopf bifurcation. Note that the crossing of these two branches of solution appears to coincide with the one of the Hopf bifurcation points, however, this seems to be purely accidental. The branch of non-homogeneous steady solutions, which become unstable at the Hopf bifurcation undergo further bifurcations, first through a pitchfork bifurcation to further unstable branches. These then undergo saddle-node bifurcations producing branches of stable patterns.

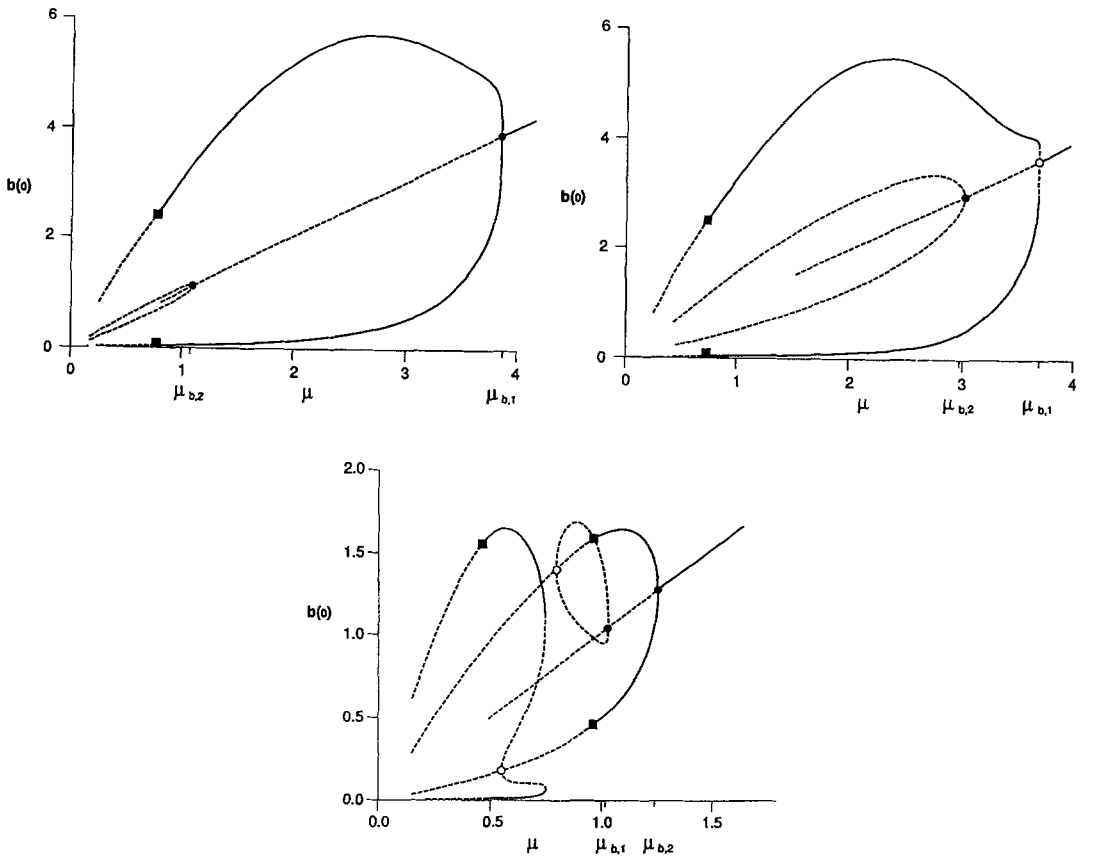

Fig. 6. Bifurcation diagrams when the first two modes k_1 and k_2 become unstable (a) $D = 0.01$, $\lambda_a \pi^2 = 24.4$, where $\mu_{b,1} > \mu_{b,2}$ and the bifurcation at $\mu = \mu_{b,1}$ is supercritical. (b) $D = 0.01$, $\lambda_a \pi^2 = 20.0$, where $\mu_{b,1} > \mu_{b,2}$ and the bifurcation at $\mu = \mu_{b,1}$ is subcritical. (c) $D = 0.1$, $\lambda_a \pi^2 = 1.4$, where $\mu_{b,2} > \mu_{b,1}$ and the bifurcation at $\mu = \mu_{b,2}$ is supercritical. (The nomenclature is the same as for Figure 6.)

To complete the discussion we consider the stable, spatially non-uniform, periodic solutions which are generated at the supercritical Hopf bifurcation. We fix attention on the first case discussed (Figure 5, with $D = 0.01$, $\lambda_a \pi^2 = 42.25$, with $\mu_{H,1} = 0.87995$). Similar behaviour was found in the other cases considered. These periodic solution branches were followed numerically still using the path-following PATH and a graph of the maximum amplitude reached by $b(0, t)$ is shown in Figure 7. This graph shows typical Hopf bifurcation behaviour for values of μ close to $\mu_{H,1}$. However, as μ is decreased away from $\mu_{H,1}$ the amplitude grows and eventually the periodic behaviour breaks down and the conversion state C (*i.e.* $a \sim \mu t$, $b \to 0$) is the only configuration left. The shape of the graph shown in Figure 7 is very similar to the equivalent one for the well-stirred system, [16].

We examined these periodic solutions in more detail by obtaining numerical solutions of the original initial-value problem (14) with initial conditions that reflected the steady, though now unstable, solution at that value of μ. The results are shown in Fig. 8 for a range of values of μ; with values of b being given at $x = 0.0$ (0.2) 1.0. The graphs are shown after the transients had died away. The large difference in amplitude between b at $x = 0.0$, and at $x = 1.0$ arises from the asymmetry in the initial conditions through the asymmetry in the steady (unstable) solution. (Note that the system is symmetric about $x = \frac{1}{2}$; the transformation $x \to 1 - x$

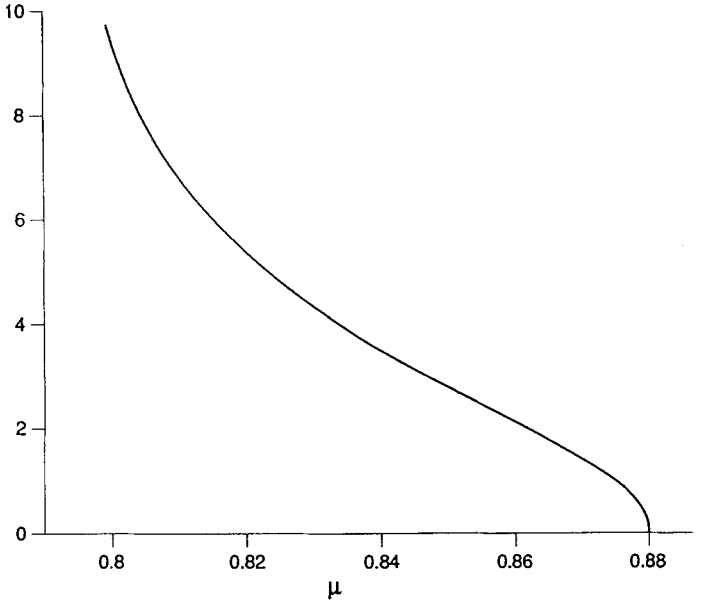

Fig. 7. A graph of the maximum amplitude of $b(0,t)$ for the spatially non-uniform periodic solutions emerging at $\mu_{H,1} = 0.87995$ (with $D = 0.01$, $\lambda_a \pi^2 = 42.24$).

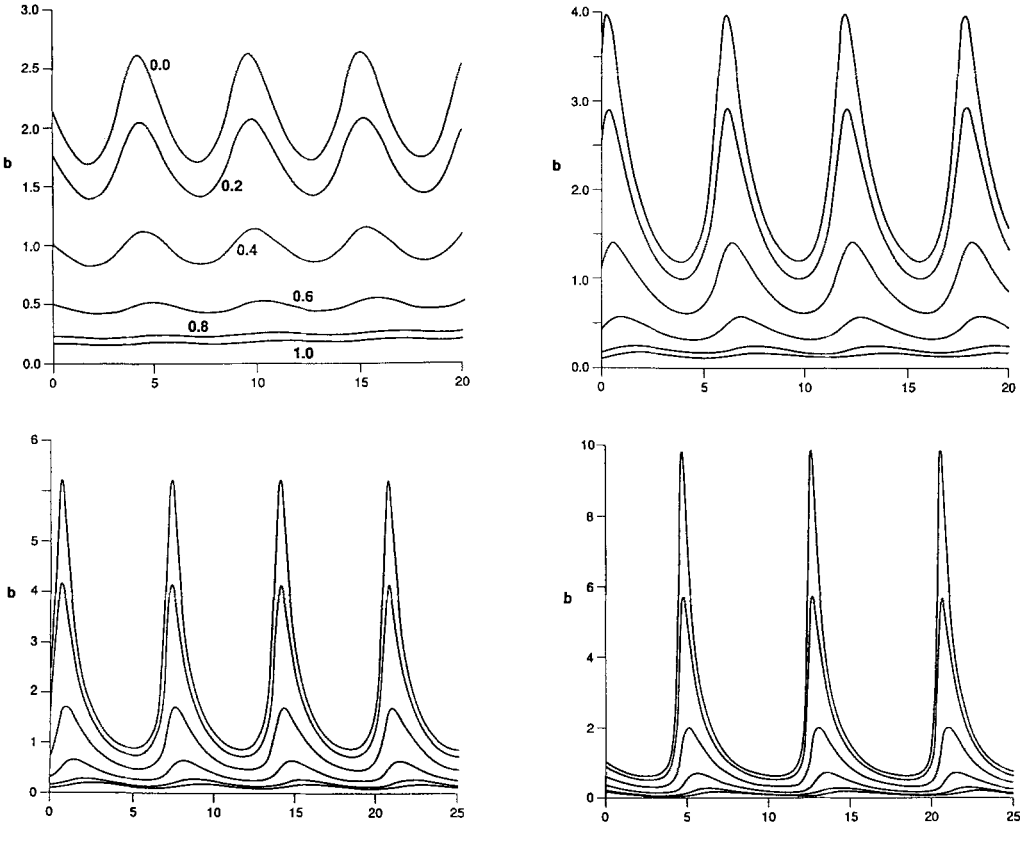

Fig. 8. Graphs of the oscillatory solutions for b at $x = 0.0, 0.2, 0.4, 0.6, 0.8, 1.0$ with (a) $\mu = 0.875$, (b) $\mu = 0.85$, (c) $\mu = 0.82$, (d) $\mu = 0.80$.

leaves (14) invariant). For $\mu = 0.875$ the oscillations are in phase with the same amplitude variation, giving rise to a 'solid body' type oscillatory behaviour. However, as μ is decreased, the oscillations become increasingly out of phase (and grow in amplitude). This can be seen most clearly in Figs. 8c, ($\mu = 0.82$) and 8d ($\mu = 0.80$). In all the cases we considered we found no secondary bifurcations of these periodic solutions, which remained with a single period throughout.

References

1. P. Gray, Review lecture: Instabilities and oscillations in chemical reactions in closed and open systems. *Proc. R. Soc. Lond.* A415 (1988) 1–34.
2. A. Hanna, A. Saul and K. Showalter, Detailed studies of propagating fronts in the iodate oxidation of arsenous acid. *J. American Chemical Soc.* 104 (1982) 3838–3844.
3. A. Saul and K. Showalter, Propagating reaction-diffusion fronts, In: R.J. Field and M. Burger (eds.), *Oscillations and Travelling Waves in Chemical Systems*. New York, (1984).
4. J. Schnakenberg, Simple chemical reaction systems with limit cycle behaviour. *J. Theoretical Biology* 81 (1979), 389–400.
5. J.D. Murray, Parameter space for Turing instability in reaction-diffusion mechanisms: a comparison of models. *J. Theoretical Biology* 98 (1982) 143–163.
6. J.D. Murray, *Mathematical Biology*. Berlin, Springer-Verlag (1989).
7. P. Arcuri and J.D. Murray, Pattern sensitivity to boundary and initial conditions in reaction-diffusion models. *J. Math. Biology* 24 (1986), 141–165.
8. E.E. Sel'kov, Self-oscillations in glycolysis. *European J. Biology* 4 (1968) 79–86.
9. A. D'Anna, P.G. Lignola and S.K. Scott, The application of singularity theory to isothermal autocatalytic open systems. *Proc. R. Soc. Lond.* A403 (1986) 341–363.
10. P. Gray and S.K. Scott, Autocatalytic reactions in the isothermal continuous stirred tank reactor: isolas and other forms of multistability. *Chemical Engineering Science* 38 (1983) 29–43.
11. P. Gray and S.K. Scott, Autocatalytic reactions in the isothermal continuous stirred tank reactor: oscillations in the system A + 2B → 3B, B → C. *Chemical Engineering Science* 39 (1984) 1087–1097.
12. P. Gray and S.K. Scott, Sustained oscillations and other exotic patterns of behaviour in isothermal reactions. *J. Physics and Chemistry* 89 (1985) 22–32.
13. P. Gray and S.K. Scott, *Chemical oscillations and unstabilities*. Oxford, Clarendon Press (1991).
14. B.F. Gray and M.J. Roberts, An analysis of chemical kinetic systems over the entire parameter space: II isothermal oscillations. *Proc. R. Soc. Lond* A416 (1988) 403–424.
15. J.H. Merkin, D.J. Needham and S.K. Scott, Oscillatory chemical reactions in closed vessels. *Proc. R. Soc. Lond* A406 (1986) 299–323.
16. J.H. Merkin, D.J. Needham and S.K. Scott, On the creation, growth and extinction of oscillatory solutions for a simple pooled chemical reaction scheme. *S.I.A.M. J. Appl. Math.* 47 (1987) 1040–1060.
17. J.H. Merkin, D.J. Needham and S.K. Scott, On the structural stability of a simple pooled chemical system. *J. Engineering Math.* 21 (1987) 115–127.
18. J.H. Merkin and D.J. Needham, Reaction-diffusion in a simple pooled chemical system. *Dynamics and Stability of Systems* 4 (1989) 141–167.
19. D.J. Needham and J.H. Merkin, Pattern formation through reaction and diffusion in a simple pooled-chemical system. *Dynamics and Stability of Systems* 4 (1989) 259–284.
20. A.H. Nayfeh, *Perturbation Methods*. New York, Wiley-Interscience (1983).
21. J.F.G. Auchmuty and G. Nicolis, Bifurcation analysis of nonlinear reaction – diffusion equations – I. evolution equations and the steady state solutions. *Bull. Math. Biology* 37 (1975) 232–365.
22. D.G. Schaeffer and M.A. Golubitsky, Bifurcation analysis near a double eigenvalue of a model chemical reaction. *Archive for Rational Mechanics and Analysis* 74 (1981) 315–347.
23. L. Bauer, H.B. Keller and E.L. Reiss, Multiple eigenvalues lead to secondary bifurcation. *S.I.A.M. Review* 17 (1975) 101–122.
24. C. Canuto, M.Y. Hussaini, A. Quarteroni and T.A. Zang, *Spectral Methods in Fluid Mechanics*. Berlin, Springer-Verlag (1987).
25. C. Kaas-Petersen, PATH-users guide. *CNLS (LEEDS) report* (1987).
26. J.C. Eilbeck, The pseudo-spectral method and path following in reaction-diffusion bifurcation studies. *S.I.A.M. J. Sci. Stat. Comput.* 7 (1986) 599–610.